

# Electronic Structure Modulation in Cationic Boron Formazanate Complexes

Ryan R. Maar<sup>†</sup>, Benjamin D. Katzman<sup>†</sup>, Paul D. Boyle, Viktor N. Staroverov, and Joe B. Gilroy<sup>\*[a]</sup>

[a] Dr. R. R. Maar, B. D. Katzman, Dr. P. D. Boyle, Prof. Dr. V. N. Staroverov, and Prof. Dr. J. B. Gilroy  
Department of Chemistry and The Centre for Advanced Materials and Biomaterials Research (CAMBR)  
The University of Western Ontario  
1151 Richmond Street North, London, Ontario N6A 5B7 (Canada)  
E-mail: joe.gilroy@uwo.ca

<sup>†</sup> These authors contributed equally to this work.

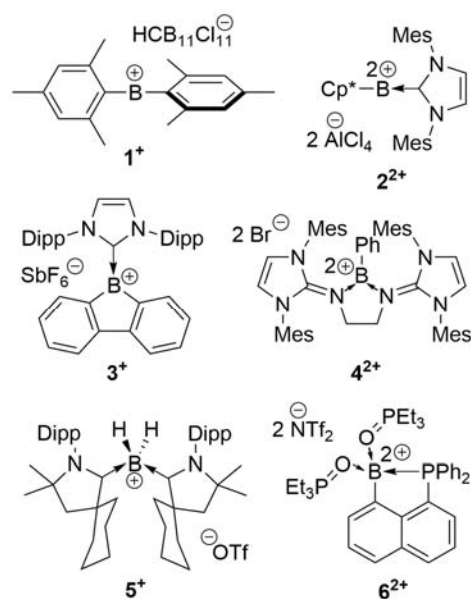
Supporting information for this article is given via a link at the end of the document.

**Abstract:** Incorporation of cationic boron atoms into molecular frameworks is an established strategy for creating chemical species with unusual bonding and reactivity but is rarely thought of as a way of enhancing molecular optoelectronic properties. We have synthesized a series of boron formazanate complexes with the aim to demonstrate that the wavelengths, intensities, and type of the first electronic transitions in BN heterocycles can be modulated by varying the cationic charge, coordination number, and supporting ligands at the boron atom. UV-vis absorption spectroscopy measurements and density-functional calculations show that these modulations are caused by changes in the geometry and extent of  $\pi$ -conjugation of the boron formazanate ring. These findings offer general guiding principles for the design of optoelectronic materials based on  $\pi$ -conjugated heterocycles containing boron and other main-group elements.

The ability of main-group elements to form stable compounds with unusual structure, bonding, and reactivity has powered a resurgence of synthetic main-group chemistry<sup>[1]</sup> and challenged the supremacy of transition metals in catalysis,<sup>[2]</sup> bond-<sup>[3]</sup> and small-molecule activation techniques,<sup>[4]</sup> and the development of functional materials.<sup>[5]</sup> In the field of functional materials in particular, incorporation of main-group elements into  $\pi$ -conjugated frameworks is becoming a powerful strategy for the development of new optoelectronic materials.<sup>[6]</sup>

Owing to its electron-deficient nature, boron is often combined with organic fragments to modulate the energies of the frontier orbitals. The resulting compounds have been suggested as promising candidates for use in organic electronics.<sup>[7]</sup> To modulate the optoelectronic properties of these molecules, suitable methods to enhance Lewis acidity at the boron centre are required. The traditional approaches rely on installing anti-aromatic scaffolds around boron atoms<sup>[8],[9]</sup> or using electron-withdrawing substituents.<sup>[10]</sup> Another strategy consists in varying the charge and coordination number of boron atoms<sup>[11]</sup> and produces two-,<sup>[12],[13]</sup> three-,<sup>[14],[15]</sup> and four-coordinate<sup>[16],[17]</sup> cations and dications such as  $1^+$ - $6^{2+}$ .<sup>[11a],[18]</sup> The method of charge variation is familiar within the catalysis arena<sup>[19]</sup> and fundamental research on the structure and bonding of cationic boron compounds<sup>[20]</sup> but remains relatively unexplored in the field of optoelectronic materials.

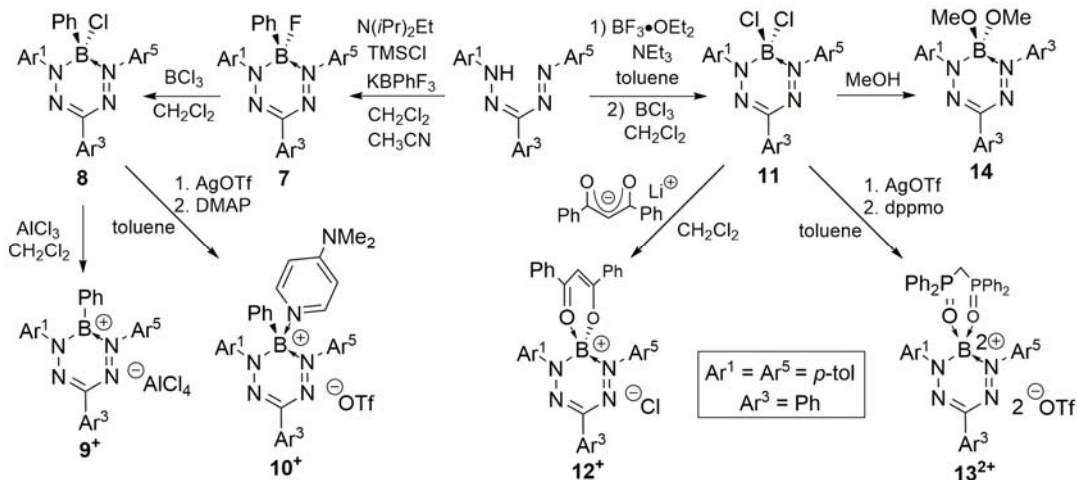
One extremely useful platform for developing the chemistry of main-group elements is furnished by formazanate ligands.<sup>[21],[22]</sup> Boron difluoride formazanate complexes display easily tunable optoelectronic properties<sup>[23]</sup> and find numerous applications as cell-imaging agents,<sup>[24]</sup> electrochemiluminescent



emitters,<sup>[23e],[25]</sup> and precursors to a wide variety of BN heterocycles with unprecedented structure and functionality.<sup>[26]</sup>

Here, we demonstrate that the variation of cationic charge and coordination number of boron atoms is a very effective approach for tuning the electronic structure and optical properties of boron formazanate complexes such as **7–14**. This demonstration is the first of its kind for BN heterocycles and can be extended to other main-group elements and similar ligand families (e.g., dipyrin, aza-dipyrin, and  $\beta$ -diketiminates).

Boron formazanate adducts **7–10**<sup>+</sup>, **12**<sup>2+</sup>, and **13**<sup>2+</sup> were synthesized according to Scheme 1 and characterized using multinuclear NMR, FT-IR, and UV-Vis absorption spectroscopies, as well as high-resolution mass spectrometry (Figures S1–S24). BPhF formazanate **7** was prepared by heating 1,5-(*p*-tolyl)-3-phenylformazan at 60 °C with excess *N*(*i*Pr)<sub>2</sub>Et and a mixture of TMSCl and KBPhF<sub>3</sub> in CH<sub>2</sub>Cl<sub>2</sub>/CH<sub>3</sub>CN for 36 h. The crude product was purified via column chromatography to produce complex **7** in 75% yield. This transformation was accompanied by a colour change from red to purple, a loss of the NH resonance in the <sup>1</sup>H NMR spectrum of 1,5-(*p*-tolyl)-3-phenylformazan ( $\delta$  = 15.51), and the appearance of broad singlets at 2.9 ppm in the <sup>11</sup>B{<sup>1</sup>H} NMR spectrum and –164.6 ppm in the <sup>19</sup>F NMR spectrum of **7**. Halide exchange between complex **7** and BCl<sub>3</sub> afforded BPhCl formazanate **8** as a dark-purple solid in quantitative yield. This was confirmed by



**Scheme 1.** Syntheses of boron formazanates 7–14. DMAP = 4-dimethylaminopyridine, OTf = trifluoromethanesulfonate, dppmo = bis(diphenylphosphino)methane dioxide.

the presence of a singlet at 2.4 ppm in the  $^{11}\text{B}\{^1\text{H}\}$  NMR spectrum and absence of signals in the  $^{19}\text{F}$  NMR spectrum for complex **8**. BPhCl formazanate **8** was converted to the three-coordinate (borenium) cation **9**<sup>+</sup> by treatment with an equimolar amount of  $\text{AlCl}_3$  in  $\text{CH}_2\text{Cl}_2$ . Complex **9**<sup>+</sup> was isolated as an air- and moisture-sensitive dark-purple solid in 98% yield. The presence of a three-coordinate boron centre was confirmed by a broad signal centred at 35.5 ppm in the  $^{11}\text{B}\{^1\text{H}\}$  NMR spectrum and a sharp singlet at 103.6 ppm in the  $^{27}\text{Al}\{^1\text{H}\}$  NMR spectrum indicative of an  $[\text{AlCl}_4]^-$  counterion. BPhCl formazanate **8** was also used to synthesize the four-coordinate (boronium) cation **10**<sup>+</sup> via treatment with AgOTf (OTf = trifluoromethanesulfonate) followed by the addition of one equivalent of 4-dimethylaminopyridine (DMAP). The resulting dark-red solid was isolated in 92% yield and displayed a broad singlet in the  $^{11}\text{B}\{^1\text{H}\}$  NMR centred at 1.9 ppm and a sharp singlet in the  $^{19}\text{F}$  NMR spectrum at  $-77.5$  ppm. Attempts to prepare **10**<sup>+</sup> by the addition of DMAP to **9**<sup>+</sup> resulted in the regeneration of **8** and  $\text{DMAP} \cdot \text{AlCl}_3$ .

$\text{BCl}_2$  formazanate **11**<sup>[26c]</sup> served as a precursor to complexes **12**<sup>+</sup>, **13**<sup>2+</sup>, and **14**, the last of which has been reported previously.<sup>[26c]</sup> Complex **11** was converted to the four-coordinate boronium cation **12**<sup>+</sup> by treatment with lithium dibenzoylmethanate in  $\text{CH}_2\text{Cl}_2$  and isolated as a red solid in 94% yield after recrystallization. Treatment of  $\text{BCl}_2$  formazanate **11** with two equivalents of AgOTf, followed by the addition of bis(diphenylphosphino)methane dioxide (dppmo), afforded a phosphine oxide-stabilized boron dication **13**<sup>2+</sup> as an orange powder in 88% yield. The  $^{11}\text{B}\{^1\text{H}\}$  NMR spectra for **12**<sup>+</sup> and **13**<sup>2+</sup> were centred at 1.9 and 0.0 ppm, respectively. The latter also displayed sharp singlets in the  $^{19}\text{F}$  and  $^{31}\text{P}\{^1\text{H}\}$  NMR spectra ( $^{19}\text{F}$ :  $-78.2$  ppm;  $^{31}\text{P}\{^1\text{H}\}$ : 54.9 ppm).

Single crystals of complexes **8**, **9**<sup>+</sup>, **12**<sup>+</sup>, and **13**<sup>2+</sup> were analyzed by X-ray diffraction (Figure 1 and Tables S1 and S2). The C-N and N-N bond lengths in complexes **8**, **9**<sup>+</sup>, **12**<sup>+</sup>, and **13**<sup>2+</sup> range from 1.334(7) to 1.356(7) Å and 1.307(2) to 1.325(6) Å, respectively. These values fall in between the standard lengths of the respective single and double bonds, suggesting that the  $\pi$  electrons of the formazanate backbone are delocalized.<sup>[27]</sup> Borenium cation **9**<sup>+</sup> in particular features a markedly shorter

average B-N bond length of 1.451(4) Å compared to complexes **8**, **12**<sup>+</sup>, and **13**<sup>2+</sup> [1.545(5) Å]. This length reduction suggests a bond order greater than 1 and can be linked to the fact that **9**<sup>+</sup> possesses an  $sp^2$ -hybridized boron atom capable of participating

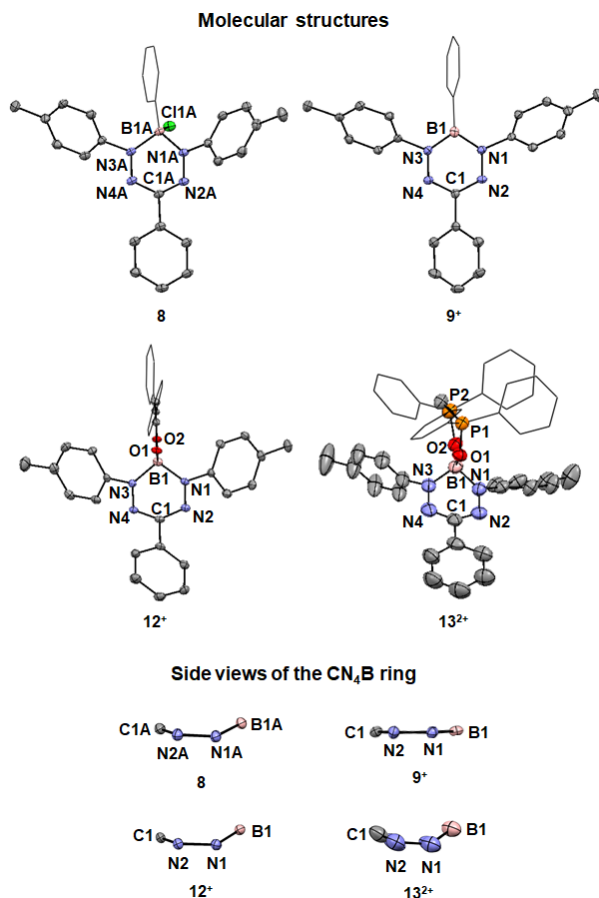


**Figure 1.** Experimental solid-state structures of four crystallized boron formazanate complexes. For clarity, hydrogen atoms are omitted and phenyl groups are shown as wireframes.

in  $\pi$ -electron delocalization via resonance. Further analysis revealed that the  $sp^3$ -hybridized boron atoms in complexes **8**, **12<sup>+</sup>**, and **13<sup>2+</sup>** are displaced from the plane defined by the four nitrogen atoms of the formazanate backbones (N1, N2, N3, N4) by a minimum of 0.380(3) Å, whereas the boron atom in complex **9<sup>+</sup>** lies within 0.041(4) Å of that plane. The planes defined by the *N*-aryl substituents and the four nitrogen atoms of the formazanate ligand are offset by at least 48.59(7)° in **8**, **9<sup>+</sup>**, **12<sup>+</sup>**, and **13<sup>2+</sup>**. Thus, the boron formazanate (CN<sub>4</sub>B) ring is almost planar in **9<sup>+</sup>** and has a boat-like conformation in the other three complexes (Figure 1).

UV-vis absorption spectroscopy data for **8–10<sup>+</sup>** (in toluene) and **12<sup>+</sup>–14** (in CH<sub>2</sub>Cl<sub>2</sub>) are presented in Figure 2a and Table 1. The choice of solvent was determined by the stability and solubility of each compound. Complexes **8**, **9<sup>+</sup>**, and **10<sup>+</sup>** exhibit broad absorption bands with molar extinction coefficients ( $\epsilon$ ) ranging from 6300 to 12100 M<sup>-1</sup> cm<sup>-1</sup>. Complex **8**, which features a four-coordinate neutral boron atom, has a maximum absorption wavelength ( $\lambda_{\text{max}}$ ) of 521 nm ( $\epsilon = 12100$  M<sup>-1</sup> cm<sup>-1</sup>), consistent with other neutral four-coordinate boron adducts of formazanates.<sup>[23a, 23b]</sup> The low-energy absorption band of **10<sup>+</sup>**, a molecule with a four-coordinate cationic boron atom, is moderately blue-shifted and has a lower intensity relative to the neutral BPhCl adduct **8** ( $\lambda_{\text{max}} = 510$  nm,  $\epsilon = 8300$  M<sup>-1</sup> cm<sup>-1</sup>). By contrast, the low-energy absorption band of three-coordinate

boron cation **9<sup>+</sup>** is strongly red-shifted ( $\lambda_{\text{max}}$  of 597 nm,  $\epsilon = 6300$  M<sup>-1</sup> cm<sup>-1</sup>) relative to complexes **8** and **10<sup>+</sup>**. The magnitudes of these shifts indicate that the coordination number of the cationic boron centres can exert a strong influence on the position of the lowest-energy absorption maximum. Complexes **14**, **12<sup>+</sup>**, and **13<sup>2+</sup>** feature  $\lambda_{\text{max}}$  values of 549 nm ( $\epsilon = 18000$  M<sup>-1</sup> cm<sup>-1</sup>), 540 nm ( $\epsilon = 5900$  M<sup>-1</sup> cm<sup>-1</sup>), and 505 nm ( $\epsilon = 9400$  M<sup>-1</sup> cm<sup>-1</sup>), respectively. This suggests that the lowest excitation energies of boron formazanate complexes with a fixed coordination number increase with increasing positive charge at boron.

To gain a better understanding of these observations, we investigated complexes **8–10<sup>+</sup>** and **12<sup>+</sup>–14** using approximate density-functional theory (DFT). The computational methodology is documented in the Supporting Information; the results are summarized in Table 1 and Figures 2b and S25. The calculations show that, in all cases, the dominant orbital pair associated with the lowest-energy electronic absorption band involves the highest occupied molecular orbital (HOMO) and the lowest unoccupied molecular orbital (LUMO). All of the lowest-energy excitations in **8–10<sup>+</sup>** and **12<sup>+</sup>–14** are of  $\pi \rightarrow \pi^*$  type (Figure 2b). Among the six complexes **8–10<sup>+</sup>** and **12<sup>+</sup>–14**, only one (**9<sup>+</sup>**) has a flat six-membered CN<sub>4</sub>B ring, while in the other five the same ring is in a boat-like conformation. The difference is clearly seen both in the experimental (Figure 1) and calculated geometries of these complexes.

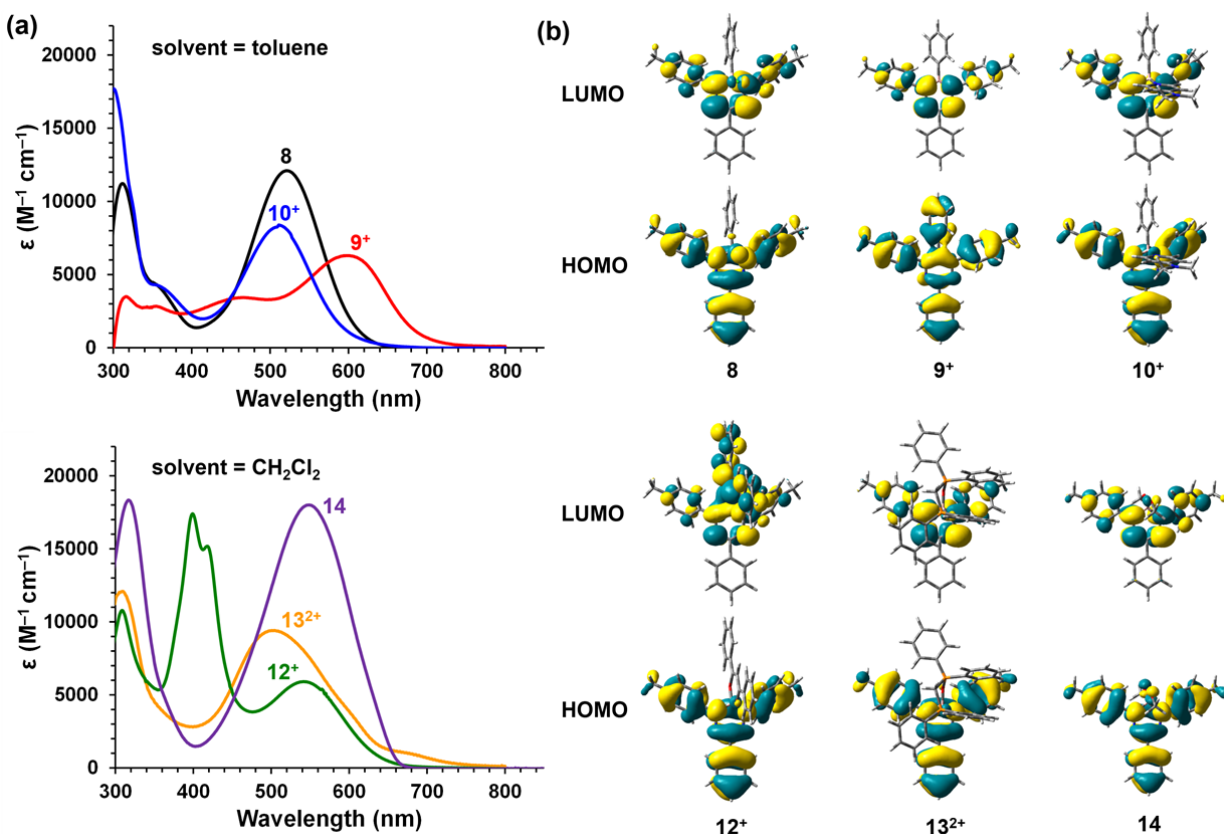


**Figure 2.** (a) UV-vis absorption spectra of 10<sup>-6</sup> M dry degassed solutions of complexes **8–10<sup>+</sup>** and **12<sup>+</sup>–14**. (b) Frontier molecular orbitals of complexes **8–10<sup>+</sup>** and **12<sup>+</sup>–14**.

**Table 1.** Experimental and simulated spectroscopic properties of complexes **8–10\*** and **12\*–14** in solution. The theoretical values were calculated by time-dependent DFT using the PBE1PBE/DGDZVP2 SCRF=CPCM method.

Complex	Supporting ligands at boron	Solvent	Experiment		Theory		
			$\lambda_{\max}$ (nm)	$\epsilon$ ( $M^{-1} \text{ cm}^{-1}$ )	$\lambda_{\max}$ (nm)	Intensity	Transition
<b>8</b>	Ph, Cl	toluene	521	12100	507	0.417	HOMO→LUMO
<b>9*</b>	Ph	toluene	597	6300	637	0.259	HOMO→LUMO
<b>10*</b>	Ph, DMAP	toluene	510	8300	502	0.401	HOMO→LUMO
<b>12*</b>	dibenzoylmethanate	CH <sub>2</sub> Cl <sub>2</sub>	540	5900	569	0.134	HOMO→LUMO
<b>13<sup>2+</sup></b>	dppmo	CH <sub>2</sub> Cl <sub>2</sub>	505	9400	514	0.308	HOMO→LUMO
<b>14</b>	(OMe) <sub>2</sub>	CH <sub>2</sub> Cl <sub>2</sub>	549	18000	546	0.500	HOMO→LUMO

The four-coordinate complexes **8** and **10\*** have nearly identical geometries of the CN<sub>4</sub>B ring, almost superimposable HOMOs and LUMOs (Figure 2b), and approximately equal  $\lambda_{\max}$  values. The modest 11 nm blue shift exhibited by **10\*** relative to **8** (in toluene) may be attributed to the positive charge of the boron atom. The three-coordinate complex **9\*** has the same +1 charge at boron as **10\*** but a much greater  $\lambda_{\max}$  value (a red shift by 76 nm) and a lower intensity of the first transition. The most plausible reason for this dramatic red shift is the flat geometry of the CN<sub>4</sub>B ring in **9\***, which enables the HOMO to extend into the phenyl substituent at boron and reduces the HOMO–LUMO gap. The three four-coordinate complexes **12\*–14** have similar nonplanar CN<sub>4</sub>B rings and look-alike HOMOs. As a result, the maximum absorption wavelengths in this set vary over a narrower range (44 nm in CH<sub>2</sub>Cl<sub>2</sub>) and are strictly correlated with the charges at boron:  $\lambda_{\max}(\mathbf{14}) > \lambda_{\max}(\mathbf{12}^*) > \lambda_{\max}(\mathbf{13}^{2+})$ .

Closer examination of the HOMO–LUMO pairs for complexes **8–10\*** and **12\*–14** suggests that the lowest-energy transitions in two of them, **9\*** and **12\***, must be accompanied by partial charge transfer between the boron formazanate rings and supporting ligands at boron. This conclusion is supported by the substantial overestimation of the calculated  $\lambda_{\max}$  values for **9\*** and **12\*** relative to experiment (Table 1) because standard density functional such as PBE1PBE are known to underestimate the energies of charge-transfer excitations.<sup>[28]</sup> These results show that supporting ligands at boron can alter not only the wavelength but also the type of low-energy electronic transitions.

In summary, we have synthesized a series of boron-based cations supported by formazanate ligands with the aim to investigate the influence of charge and coordination number at boron on the electronic properties of BN heterocycles. Our conclusions are as follows: i) an increase in the cationic charge on boron in four-coordinate compounds (e.g., **10\*** and **13<sup>2+</sup>**) blue-shifts  $\lambda_{\max}$  and decreases the intensities of the lowest-energy absorption bands; ii) introduction of a planar, 3-coordinate cationic boron atom (as in **9\***) extends  $\pi$ -conjugation in the HOMO and dramatically red-shifts  $\lambda_{\max}$ ; iii) chelating  $\pi$ -conjugated supporting ligands (as in **12\***) reorganize the electronic structure and red-shift  $\lambda_{\max}$  by inducing charge transfer. Collectively, this work establishes guiding principles for the design of optoelectronic molecular materials featuring cationic boron fragments that can be applied to  $\pi$ -conjugated heterocycles containing other main-group elements.

## Acknowledgements

This work was supported by the Natural Sciences and Engineering Research Council (NSERC) of Canada (V.N.S.: DG, RGPIN-2020-06420; J.B.G.: DG, RGPIN-2018-04240, R.R.M.: CGS-D Scholarship), the Ontario Ministry of Research and Innovation (J.B.G.: ERA, ER-14-10-147), and the Canadian Foundation for Innovation (J.B.G.: JELF, 33977).

**Keywords:** Borenium, boronium, formazanate ligands, BN heterocycles, optoelectronic materials.

- [1] R. L. Melen, *Science* **2019**, *363*, 479–484.
- [2] J. Lam, K. M. Szkop, E. Mosaferi, D. W. Stephan, *Chem. Soc. Rev.* **2019**, *48*, 3592–3612.
- [3] T. Chu, G. I. Nikonov, *Chem. Rev.* **2018**, *118*, 3608–3680.
- [4] G. C. Welch, R. R. S. Juan, J. D. Masuda, D. W. Stephan, *Science* **2006**, *314*, 1124–1126.
- [5] T. Baumgartner, F. Jäkle, *Main Group Strategies towards Functional Hybrid Materials*, Wiley, Chichester, **2018**.
- [6] M. Hirai, N. Tanaka, M. Sakai, S. Yamaguchi, *Chem. Rev.* **2019**, *119*, 8291–8331.
- [7] a) F. Jäkle, *Chem. Rev.* **2010**, *110*, 3985–4022; b) L. Ji, S. Griesbeck, T. B. Marder, *Chem. Sci.* **2017**, *8*, 846–863; c) S. K. Mellerup, S. Wang, *Trends in Chemistry* **2019**, *1*, 77–89.
- [8] H. Braunschweig, T. Kupfer, *Chem. Commun.* **2011**, *47*, 10903–10914.
- [9] a) A. Y. Houghton, J. Hurmalainen, A. Mansikkamäki, W. E. Piers, H. M. Tuononen, *Nat. Chem.* **2014**, *6*, 983–988; b) Z. Zhang, R. M. Edkins, M. Haehnel, M. Wehner, A. Eichhorn, L. Mailänder, M. Meier, J. Brand, F. Brede, K. Müller-Buschbaum, H. Braunschweig, T. B. Marder, *Chem. Sci.* **2015**, *6*, 5922–5927; c) J. H. Barnard, S. Yruegas, K. Huang, C. D. Martin, *Chem. Commun.* **2016**, *52*, 9985–9991.
- [10] I. B. Sivaev, V. I. Bregadze, *Coord. Chem. Rev.* **2014**, *270–271*, 75–88.
- [11] a) W. Yang, K. E. Krantz, L. A. Freeman, D. A. Dickie, A. Molino, A. Kaur, D. J. D. Wilson, R. J. Gilliard Jr., *Chem. Eur. J.* **2019**, *25*, 12512–12516; b) Y. Adachi, F. Arai, F. Jäkle, *Chem. Commun.* **2020**, *56*, 5119–5122.
- [12] a) T. Scherpf, K.-S. Feichtner, V. H. Gessner, *Angew. Chem. Int. Ed.* **2017**, *56*, 3275–3279; b) N. Tanaka, Y. Shoji, D. Hashizume, M. Sugimoto, T. Fukushima, *Angew. Chem. Int. Ed.* **2017**, *56*, 5312–5316; c) H.-C. Tseng, C.-T. Shen, K. Matsumoto, D.-N. Shih, Y.-H. Liu, S.-M. Peng, S. Yamaguchi, Y.-F. Lin, C.-W. Chiu, *Organometallics* **2019**, *38*, 4516–4521.
- [13] W.-H. Lee, Y.-F. Lin, G.-H. Lee, S.-M. Peng, C.-W. Chiu, *Dalton Trans.* **2016**, *45*, 5937–5940.
- [14] a) C. Bonnier, W. E. Piers, M. Parvez, T. S. Sorensen, *Chem. Commun.* **2008**, 4593–4595; b) E. Tsurumaki, S.-y. Hayashi, F. S. Tham, C. A. Reed, A. Osuka, *J. Am. Chem. Soc.* **2011**, *133*, 11956–11959; c) D. Franz, E. Irran, S. Inoue, *Angew. Chem. Int. Ed.* **2014**, *53*, 14264–

- 14268; d) M. Devillard, R. Brousses, K. Miqueu, G. Bouhadir, D. Bourissou, *Angew. Chem. Int. Ed.* **2015**, *54*, 5722–5726; e) J. M. Farrell, D. W. Stephan, *Angew. Chem. Int. Ed.* **2015**, *54*, 5214–5217; f) J. A. B. Abdalla, R. C. Tirfoin, H. Niu, S. Aldridge, *Chem. Commun.* **2017**, *53*, 5981–5984; g) Y. K. Loh, K. Porteous, M. Á. Fuentes, D. C. H. Do, J. Hicks, S. Aldridge, *J. Am. Chem. Soc.* **2019**, *141*, 8073–8077; h) T. Janes, Y. Diskin-Posner, D. Milstein, *Angew. Chem. Int. Ed.* **2020**, *59*, 4932–4936; i) T. Heitkemper, C. Sindlinger, *Chem. Eur. J.* **2020**, *26*, 11684–11689.
- [15] W.-C. Chen, C.-Y. Lee, B.-C. Lin, Y.-C. Hsu, J.-S. Shen, C.-P. Hsu, G. P. A. Yap, T.-G. Ong, *J. Am. Chem. Soc.* **2014**, *136*, 914–917.
- [16] a) T. W. Hudnall, F. P. Gabbaï, *Chem. Commun.* **2008**, 4596–4597; b) A. Prokofjevs, J. W. Kampf, A. Solovyev, D. P. Curran, E. Vedejs, *J. Am. Chem. Soc.* **2013**, *135*, 15686–15689; c) L. Kong, W. Lu, Y. Li, R. Ganguly, R. Kinjo, *J. Am. Chem. Soc.* **2016**, *138*, 8623–8629; d) W. Lu, Y. Li, R. Ganguly, R. Kinjo, *Angew. Chem. Int. Ed.* **2017**, *56*, 9829–9832; e) S. Rixin Wang, M. Arrowsmith, H. Braunschweig, R. D. Dewhurst, V. Paprocki, L. Winner, *Chem. Commun.* **2017**, *53*, 11945–11947; f) S. J. Geier, C. M. Vogels, N. R. Mellonie, E. N. Daley, A. Decken, S. Doherty, S. A. Westcott, *Chem. Eur. J.* **2017**, *23*, 14485–14499; g) S. Hagspiel, M. Arrowsmith, F. Fantuzzi, A. Hermann, V. Paprocki, R. Drescher, I. Krummenacher, H. Braunschweig, *Chem. Sci.* **2020**, *11*, 551–555.
- [17] a) H. Schmidbaur, T. Wimmer, G. Reber, G. Müller, *Angew. Chem. Int. Ed. Engl.* **1988**, *27*, 1071–1074; b) D. Vidovic, M. Findlater, A. H. Cowley, *J. Am. Chem. Soc.* **2007**, *129*, 8436–8437; c) H. Braunschweig, M. Kaupp, C. Lambert, D. Nowak, K. Radacki, S. Schinzel, K. Uttinger, *Inorg. Chem.* **2008**, *47*, 7456–7458; d) G. P. McGovern, D. Zhu, A. J. A. Aquino, D. Vidović, M. Findlater, *Inorg. Chem.* **2013**, *52*, 13865–13868.
- [18] a) R. Kinjo, B. Donnadiou, M. A. Celik, G. Frenking, G. Bertrand, *Science* **2011**, *333*, 610–613; b) C.-T. Shen, Y.-H. Liu, S.-M. Peng, C.-W. Chiu, *Angew. Chem. Int. Ed.* **2013**, *52*, 13293–13297; c) Y. Shoji, N. Tanaka, K. Mikami, M. Uchiyama, T. Fukushima, *Nat. Chem.* **2014**, *6*, 498–503; d) M. Devillard, S. Mallet-Ladeira, G. Bouhadir, D. Bourissou, *Chem. Commun.* **2016**, *52*, 8877–8880; e) D. Franz, T. Szilvási, A. Pöthig, F. Deiser, S. Inoue, *Chem. Eur. J.* **2018**, *24*, 4283–4288.
- [19] P. Eisenberger, C. M. Crudden, *Dalton Trans.* **2017**, *46*, 4874–4887.
- [20] a) W. E. Piers, S. C. Bourke, K. D. Conroy, *Angew. Chem. Int. Ed.* **2005**, *44*, 5016–5036; b) D. Franz, S. Inoue, *Chem. Eur. J.* **2019**, *25*, 2898–2926.
- [21] J. B. Gilroy, E. Otten, *Chem. Soc. Rev.* **2020**, *49*, 85–113.
- [22] a) M.-C. Chang, T. Dann, D. P. Day, M. Lutz, G. G. Wildgoose, E. Otten, *Angew. Chem. Int. Ed.* **2014**, *53*, 4118–4122; b) M.-C. Chang, E. Otten, *Chem. Commun.* **2014**, *50*, 7431–7433; c) R. Travieso-Puente, M.-C. Chang, E. Otten, *Dalton Trans.* **2014**, *43*, 18035–18041; d) R. Travieso-Puente, J. O. P. Broekman, M.-C. Chang, S. Demeshko, F. Meyer, E. Otten, *J. Am. Chem. Soc.* **2016**, *138*, 5503–5506; e) R. Mondol, D. A. Snoeken, M.-C. Chang, E. Otten, *Chem. Commun.* **2017**, *53*, 513–516; f) E. Kabir, C.-H. Wu, J. I.-C. Wu, T. S. Teets, *Inorg. Chem.* **2016**, *55*, 956–963; g) E. Kabir, G. Mu, D. A. Momtaz, N. A. Bryce, T. S. Teets, *Inorg. Chem.* **2019**, *58*, 11672–11683; h) D. L. J. Broere, B. Q. Mercado, P. L. Holland, *Angew. Chem. Int. Ed.* **2018**, *57*, 6507–6511; i) R. R. Maar, A. Rabiee Kenaree, R. Zhang, Y. Tao, B. D. Katzman, V. N. Staroverov, Z. Ding, J. B. Gilroy, *Inorg. Chem.* **2017**, *56*, 12436–12447; j) R. R. Maar, S. D. Catingan, V. N. Staroverov, J. B. Gilroy, *Angew. Chem. Int. Ed.* **2018**, *57*, 9870–9874.
- [23] a) S. M. Barbon, J. T. Price, P. A. Reinkeluers, J. B. Gilroy, *Inorg. Chem.* **2014**, *53*, 10585–10593; b) S. M. Barbon, V. N. Staroverov, J. B. Gilroy, *J. Org. Chem.* **2015**, *80*, 5226–5235; c) M.-C. Chang, A. Chantzis, D. Jacquemin, E. Otten, *Dalton Trans.* **2016**, *45*, 9477–9484; d) A. Melenbacher, J. S. Dhindsa, J. B. Gilroy, M. J. Stillman, *Angew. Chem. Int. Ed.* **2019**, *58*, 15339–15343; e) R. R. Maar, R. Zhang, D. G. Stephens, Z. Ding, J. B. Gilroy, *Angew. Chem. Int. Ed.* **2019**, *58*, 1052–1056.
- [24] R. R. Maar, S. M. Barbon, N. Sharma, H. Groom, L. G. Luyt, J. B. Gilroy, *Chem. Eur. J.* **2015**, *21*, 15589–15599.
- [25] a) M. Hesari, S. M. Barbon, V. N. Staroverov, Z. Ding, J. B. Gilroy, *Chem. Commun.* **2015**, *51*, 3766–3769; b) M. Hesari, S. M. Barbon, R. B. Mendes, V. N. Staroverov, Z. Ding, J. B. Gilroy, *J. Phys. Chem. C* **2018**, *122*, 1258–1266.
- [26] a) M.-C. Chang, E. Otten, *Inorg. Chem.* **2015**, *54*, 8656–8664; b) S. M. Barbon, V. N. Staroverov, J. B. Gilroy, *Angew. Chem. Int. Ed.* **2017**, *56*, 8173–8177; c) R. R. Maar, N. A. Hoffman, V. N. Staroverov, J. B. Gilroy, *Chem. Eur. J.* **2019**, *25*, 11015–11019.
- [27] J. R. Rumble, *CRC Handbook of Chemistry and Physics*, 98th ed., CRC Press/Taylor and Francis, Boca Raton, FL.
- [28] a) Y. Tawada, T. Tsuneda, S. Yanagisawa, T. Yanai, K. Hirao, *J. Chem. Phys.* **2004**, *120*, 8425–8433; b) T. Yanai, D. P. Tew, N. C. Handy, *Chem. Phys. Lett.* **2004**, *393*, 51–57; c) S. Kümmel, *Adv. Energy Mater.* **2017**, *7*, 1700440.